ENVIRONMENTAL RESEARCH
WATER

PURPOSE-LED PUBLISHING™ Part of the ENVIRONMENTAL RESEARCH SERIES

PAPER • OPEN ACCESS

A multi-model assessment of global freshwater temperature and thermoelectric power supply under climate change

To cite this article: Edward R Jones *et al* 2025 *Environ. Res.: Water* **1** 025002

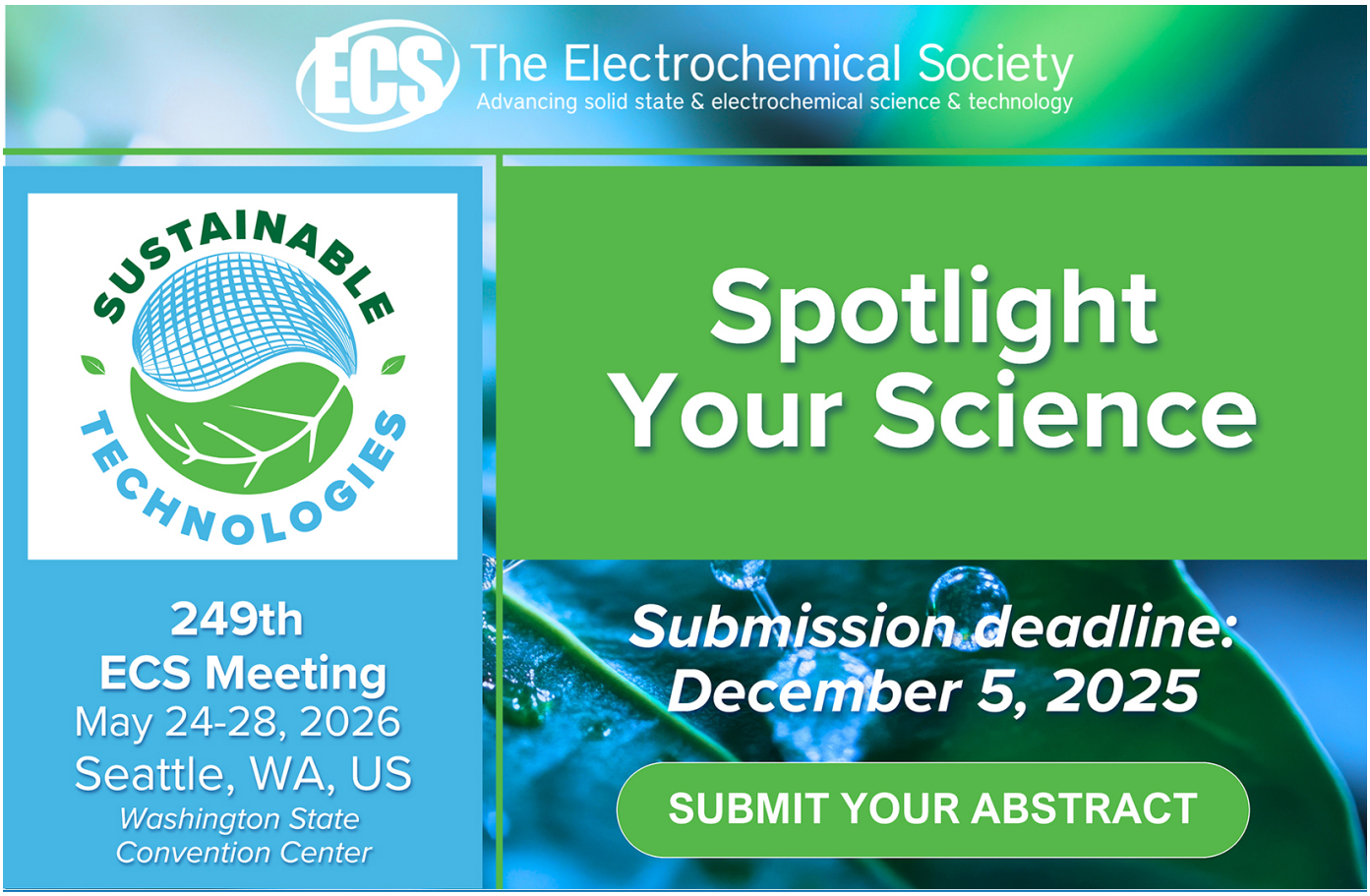

ENVIRONMENTAL RESEARCH
WATER

OPEN ACCESS

RECEIVED
27 February 2025

REVISED
8 May 2025

ACCEPTED FOR PUBLICATION
3 June 2025

PUBLISHED
25 June 2025

PAPER

A multi-model assessment of global freshwater temperature and thermoelectric power supply under climate change

Edward R Jones[1,*], Rens van Beek[1], Gabriel Cárdenas Belleza[1], Peter Burek[2], Stephen J Dugdale[3], Martina Flörke[4], Dor Fridman[2], Simon N Gosling[3], Rohini Kumar[5], Daniel Mercado-Bettin[6], Hannes Müller Schmied[7,8], Zeli Tan[9], Wim Thiery[10], Ammanuel B Tilahun[4], Niko Wanders[1] and Michelle T H van Vliet[1]

[1] Department of Physical Geography, Faculty of Geosciences, Utrecht University, Utrecht, The Netherlands
[2] Water Security Research Group, Biodiversity and Natural Resources Program, International Institute for Applied Systems Analysis, Laxenburg, Austria
[3] School of Geography, University of Nottingham, Nottingham, United Kingdom
[4] Chair of Engineering Hydrology and Water Resources Management, Ruhr University Bochum, Bochum, Germany
[5] Department Computational Hydrosystems, Helmholtz Centre for Environmental Research GmbH—UFZ, Leipzig, Germany
[6] Centre for Advanced Studies of Blanes, Spanish National Research Council, Blanes, Spain
[7] Institute of Physical Geography, Goethe University Frankfurt, Frankfurt am Main, Germany
[8] Senckenberg Leibniz Biodiversity and Climate Research Centre (SBiK-F), Frankfurt am Main, Germany
[9] Pacific Northwest National Laboratory, Richland, WA, United States of America
[10] Department of Water and Climate, Vrije Universiteit Brussel, Brussels, Belgium
[*] Author to whom any correspondence should be addressed.

E-mail: e.r.jones@uu.nl

Keywords: water temperature, climate change, multi-model ensemble, ISIMIP, CMIP, modelling

Supplementary material for this article is available online

Abstract

Water temperature is a key abiotic factor influencing aquatic ecosystem health and the services provided to both nature and humans. Global water temperature models offer possibilities to improve our understanding of water temperature regimes, which is increasingly important against the backdrop of climate change. Yet, existing studies have predominantly relied on a single model, which can lead to an incomplete representation of uncertainty and potential biases, in addition to limited insight into the range of possible future conditions, which ultimately reduces the robustness of climate impact assessments. Here, we provide a comprehensive assessment of surface freshwater temperature changes from various river and lake models for both past conditions and under future scenarios of climate change. Global models consistently simulate that surface water temperatures are currently 0.5 °C–0.8 °C higher than at the turn of the century (i.e. 1981–2000), and that warming will extend and intensify with future global change throughout the 21st century. While the strength of warming is highly sensitive to the different water temperature models, emissions scenarios and global climate models, our multi-model ensemble shows a global average annual water temperature rise of between +1.3 °C and +4.1 °C by the end of the century. To illustrate a potential societal impact of our results, we evaluate how future changes in discharge and water temperature may affect existing thermoelectric power plants, estimating average annual reductions of 1.5%–6% in global usable capacity by the end of the century. However, with river water temperatures projected to exhibit more pronounced seasonal patterns in the future—especially under the more extreme climate change scenarios and during summer months in the Northern Hemisphere—intra-annual reductions in usable capacity can be much more severe. Given the challenges associated with (large-scale) adaptation to control water temperature regimes, strong climate change mitigation is crucial for minimising water temperature rises and its associated negative impacts on humankind and ecosystems.

1. Introduction

Water temperature is a key abiotic factor for determining the health, functioning and services provided by aquatic ecosystems. Water temperature directly impacts the distribution (Wehrly *et al* 2007, Isaak *et al* 2015, Barbarossa *et al* 2021), metabolism (Liu *et al* 2019) and survival (Isaak *et al* 2018, Nicola *et al* 2018) of aquatic organisms, while also influencing human activities such as recreational activities (Wolf *et al* 2017) and water treatment (Delpla *et al* 2009, Heberling *et al* 2015). Electricity production by thermoelectric power plants is also strongly dependent on the temperature of freshwater resources, which directly affect operational efficiency (Linnerud *et al* 2011, Petrakopoulou *et al* 2020) and reduce the cooling potential per unit volume, thereby increasing overall water demand (van Vliet *et al* 2016a). Furthermore, regulatory limits on the temperature of cooling water discharges can require power plants to curtail operations, which can lead to decreased supply and increased electricity prices (Mcdermott and Nilsen 2014, van Vliet *et al* 2016b). Indirectly, water temperature strongly impacts biogeochemical processes (e.g. carbon and nutrient cycles) and water quality (e.g. oxygen solubility, toxicity of pollutants) which further impacts humans and the environment (Johnson *et al* 2024). Given these wide-ranging direct and indirect impacts, the ecological and societal benefits of improving our understanding of global water temperature dynamics are clear (Hannah and Garner 2015), particularly in the increasingly important context of anthropogenic stressors (Ficklin *et al* 2023).

While water temperature monitoring via remote sensing approaches (Martí-Cardona *et al* 2019, Tavares *et al* 2020) and high-frequency automated logger networks (Jackson *et al* 2015, Isaak *et al* 2017) are becoming increasingly common, our understanding of historic water temperature is primarily based upon traditional *in-situ* monitoring. Analysis of water temperature data records indicates that rivers (Kaushal *et al* 2010, Hannah and Garner 2015, Isaak *et al* 2017, Ptak *et al* 2019) and lakes (O'Reilly *et al* 2015, Woolway *et al* 2019, Jane *et al* 2021) are warming across the globe. However, the availability of long-term water temperature monitoring data remains limited to a relatively small number of locations (Pohle *et al* 2019, Worrall *et al* 2022, Zhu *et al* 2022). As is typical for most water quality constituents, the geographic distribution of observations is highly uneven, often discontinuous and has a strong bias towards North America, Western Europe and Australia (Ficklin *et al* 2023, Jones *et al* 2024) (figure S1; figure S2). This presents a major challenge for understanding and quantifying water temperature dynamics and its sensitivity to historical climatic changes, especially in ungauged catchments. Similarly, observational records alone are inadequate for exploring the impact of future climate, land use and anthropogenic changes on future freshwater thermal regimes.

Models offer unique opportunities to explore the spatial and temporal dynamics of water temperature beyond what is possible through monitoring efforts alone. Physically-based models aim to represent processes (e.g. solar radiation flux, heat exchange at the air-water and sediment-water interfaces, lateral (advective) transport of energy) to provide realistic estimates of water temperature. As they use physically-based equations, opposed to statistical ones, these models are particularly suitable for application in ungauged basins and provide a strong basis for modelling future water temperatures under climate change (Wanders *et al* 2019). Water temperature models have been developed and applied for past and/or future conditions across various spatial scales, from individual reaches (Garner *et al* 2014, Hall and Selker 2021) to whole streams/rivers (Baker *et al* 2018, Dugdale *et al* 2024), entire catchments (Loinaz *et al* 2013, Rincón *et al* 2023) and ultimately global applications (Vanderkelen *et al* 2020) (e.g. see models in table 1). Such studies have typically compared modelled water temperature against historical observational data to quantify model performance, before using the model to better understand current water temperature regimes or to simulate future water temperature in response to land-use or climate change (Dugdale *et al* 2018, Lee *et al* 2020, Michel *et al* 2022). With a few notable exceptions, comparisons of water temperature simulations across different models are rare—especially at the global scale (van Vliet *et al* 2016a, Grant *et al* 2021, Woolway *et al* 2021).

Here, we provide a comprehensive assessment of temperature changes in surface water bodies, including rivers and lakes, in response to changing climate conditions. To this end, we analyse both the individual responses of various water temperature models and the multi-model ensemble under past conditions and future scenarios of climate change. Our study is aligned with a large-scale modelling initiative, the Inter-Sectoral Impact Model Intercomparison Project (ISIMIP); www.isimip.org. As ISIMIP also aims to develop robust assessments of the impacts of climate change on various sectors, including the energy sector, we use a multi-model ensemble approach to estimate how future changes in water temperature could impact the viability of thermoelectric power plants located across the world.

Table 1. Full list of participating global water temperature model, future scenarios and global climate models considered in the first phase of this study.

Model	Spatial resolution	ISMIP round	Future scenarios	Global climate models	Key reference paper
ALBM	0.5° (Lakes)	ISIMIP3b	SSP1-RCP2.6; SSP3-RCP7.0; SSP5-RCP8.5	GFDL; IPSL; MPI; MRI; UKESM	(Tan *et al* 2024)
CLM45	0.5° (Lakes)	ISIMIP2b	RCP2.6; RCP6.0; RCP8.5	GFDL; HADGEM; IPSL; MIROC	(Oleson *et al* 2013)
CWatXM-WQ	5 arc-min (Rivers)	ISIMIP3b	SSP1-RCP2.6; SSP2-RCP4.5; SSP3-RCP7.0; SSP5-RCP8.5	GFDL; IPSL; MPI; MRI; UKESM	(Morrill *et al* 2005)
DyERTM	0.5° (Rivers)	ISIMIP3b	SSP1-RCP2.6; SSP3-RCP7.0; SSP5-RCP8.5	GFDL; IPSL; MPI; MRI; UKESM	(Mohseni and Stefan 1999)
DynQual	5 arc-min (Rivers)	ISIMIP3b	SSP1-RCP2.6; SSP3-RCP7.0; SSP5-RCP8.5	GFDL; IPSL; MPI; MRI; UKESM	(Jones *et al* 2023)
DynWat	5 arc-min (Rivers)	ISIMIP2b	RCP2.6; RCP4.5; RCP6.0; RCP8.5	GFDL; HADGEM; IPSL; MIROC; NORESM	(Wanders *et al* 2019)
GOTM	0.5° (Lakes)	ISIMIP3b	SSP1-RCP2.6; SSP3-RCP7.0; SSP5-RCP8.5	GFDL; IPSL; MPI; MRI; UKESM	(Umlauf and Burchard 2005)
SIMSTRAT-UOG	0.5° (Lakes)	ISIMIP2b	RCP2.6; RCP6.0; RCP8.5	GFDL; HADGEM; IPSL; MIROC	(Goudsmit *et al* 2002)
VIC-RBM	0.5° (Rivers)	ISIMIP2b	RCP2.6; RCP8.5	GFDL; HADGEM; IPSL; MIROC; NORESM	(van Vliet *et al* 2012b)
WaterGAP2.2e	0.5° (Rivers)	ISIMIP3b	SSP1-RCP2.6; SSP3-RCP7.0; SSP5-RCP8.5	GFDL; IPSL; MPI; MRI; UKESM	(Müller Schmied *et al* 2024)
WaterGAP3	5 arc-min (Rivers)	ISIMIP2b	RCP2.6; RCP6.0; RCP8.5	GFDL; HADGEM; IPSL; MIROC	(Punzet *et al* 2012)

2. Methods

2.1. Water temperature models and data analysis

Our analysis is performed in two distinct phases. In the first phase, we obtained simulations from 11 global water temperature models (7 river and 4 lake models) from ISIMIP, spanning a range of spatial resolutions (5 arc-min to 0.5°), global climate models (GCMs) and future scenarios as represented by different combinations of shared socio-economic pathways (SSPs) and representative concentration pathways (RCPs) (table 1). All models are consistently forced with CMIP5 (Taylor *et al* 2012) or CMIP6 (Eyring *et al* 2016) climate data, which are bias-corrected consistently in different phases of ISIMIP (i.e. ISIMIP2b for CMIP5 and ISIMIP3b for CMIP6). The lake models simulate water temperature for ∼17 500 (ISIMIP2) and ∼41 000 (ISIMIP3) representative lakes (Golub *et al* 2022), for which we consider surface water temperature only. Conversely, the river models simulate water temperatures for every land-based pixel. For the purpose of our large ensemble, future scenarios from ISIMIP2b and ISIMIP3b are combined based on common RCPs (e.g. simulations using RCP2.6 in ISIMIP2b are combined with simulations using SSP1-RCP2.6 in ISIMIP3b).

Using the full model suite, we investigate future water temperature anomalies at the global level. We use an area-weighted arithmetic mean approach to calculate global average water temperatures, whereby each (non-NA) simulated water temperature is weighted by the size of the grid cell it represents, in order to address differences in the spatial resolution of the water temperature models considered and the latitudinal variation in grid cell size that is present in global gridded datasets. Annual average water temperature simulations from a historic reference period (1981–2000) are compared to future projections (until 2099)

under various global change scenarios in combination with different GCMs. We demonstrate the spread in projected future water temperature anomalies arising from the different models, displaying the plausible trajectories of surface freshwater temperature rises under different assumptions of climate change. We analyse anomalies, as opposed to absolute water temperature changes, to better isolate the signal of climate change from the noise occurring due to model biases, thereby providing more robust insights into future climate change impacts on surface water temperature globally.

In the second phase, we conduct detailed analysis on global simulations from three coupled hydrological and river water temperature models (CWatM-WQ, DynQual and WaterGAP2.2e). These models are selected due to availability of daily water temperature simulations for the historical period (1980–2019) using reanalysis-based climate forcing from ISIMIP3a (Frieler *et al* 2024). Model performance is evaluated at the daily timestep with respect to 841 781 observations made at 22 990 monitoring stations located worldwide, using the Kling–Gupta efficiency (KGE), root mean square error, percent bias and coefficient of determination (R^2) (supplementary figures S3–S6). In addition to model evaluation, this analysis informs more detailed interpretation and consistent intercomparisons of simulations amongst these three river water temperature models.

Following evaluation of historic water temperature simulations from CWatM-WQ, DynQual and WaterGAP2.2e using ISIMIP3a forcing, we make detailed comparisons of future projections of monthly water temperature (up to 2100) from these models using ISIMIP3b forcing for the five primary GCMs (GDFL-ESM4, UKESM1-0-LL, MPI-ESM1-2-HR, IPSL-CM6A-LR and MRI-ESM2-0) under three future climate change scenarios (SSP1-RCP2.6, SSP3-RCP7 and SSP5-RCP8.5) (Büchner 2021).

2.2. Water temperature impacts on the thermoelectric sector

Rises in water temperature pose well-known risks to humans and the environment. To illustrate one potential impact of projected increases in water temperature on society, we estimated the usable capacity of thermoelectric power plants (from 2005 to 2100) under three different scenarios of climate change using simulations of monthly discharge and water temperature from CWatM-WQ, DynQual and WaterGAP2.2e. To this end, we adopt an approach developed and extensively described in previous work (Koch and Vögele 2009, van Vliet *et al* 2012a) (equation (1)),

$$q = W \cdot \frac{1-n_{\text{total}}}{n_{\text{elec}}} \cdot \frac{(1-\alpha)\cdot(1-\beta)\cdot\omega\cdot EZ}{\rho_{\text{w}}\cdot C_{\text{p}}\cdot\max\left(\min\left(\left(Tl_{\max}-T_{\text{river}}\right),\Delta Tl_{\max}\right),1\right)}$$

$$W_{\max} = \frac{\min\left((\gamma\cdot Q,q)\cdot\rho_{\text{w}}\cdot C_{\text{p}}\cdot\max\left(\min\left(\left(Tl_{\max}-T_{\text{river}}\right),\Delta Tl_{\max}\right),1\right)\right.}{\frac{1-n_{\text{total}}}{n_{\text{elec}}}\cdot(1-\alpha)\cdot(1-\beta)\cdot\omega\cdot EZ}. \quad (1)$$

Here, q is the estimated monthly cooling water demand ($m^3\ s^{-1}$). W represents the installed capacity of a power plant (W); η_{total}, η_{elec}, α and β are ratios representing of total efficiency, electric efficiency, the share of waste heat not discharged by cooling water (e.g. waste heat recovery) and the share of waste heat released into the air, respectively, which depend on power plant fuel type and cooling technology, originating from Platts UDI World Electric Power Plants Database (WEPP) (Platts 2012) and as described in previous studies (Raptis and Pfister 2016, van Vliet *et al* 2016a). Similarly, ω is a correction factor accounting for the effects of changes in air temperature and humidity within a year, EZ is a densification factor, λ is a correction factor accounting for the effects of changes in efficiencies, and γ is the maximum fraction of river discharge that can be withdrawn for cooling of thermoelectric power plants, which are dependent upon power plant fuel type and cooling technology, originating from Platts UDI WEPP (Platts 2012) and as described in previous studies (Raptis and Pfister 2016, van Vliet *et al* 2016a). ρ_{w} is the density of freshwater ($kg\ m^{-3}$) and C_{p} is the heat capacity of water ($J\ kg^{-1}\ °C^{-1}$). $Tl_{\max}$ is the maximum permissible temperature of the cooling water (°C), estimated as the 95th percentile of daily simulated water temperature over 1980–2019; while $\Delta Tl_{\max}$ is the maximum permissible temperature increase of the cooling water (°C), set at 7 °C following van Vliet *et al* (2016b) and Jones *et al* (2023). $W_{\max}$ is the usable capacity of a power plant (W), T_{river} is the simulated monthly mean average river temperature (°C) and Q is the simulated monthly average river discharge ($m^3\ s^{-1}$).

We apply this approach to 7,419 thermoelectric power plants, detailed in a global dataset (Lohrmann *et al* 2019). The following criteria were set for including thermoelectric power plants in our analyses: (i) use of fossil fuels (oil, gas or coal) or nuclear energy as the primary fuel type; (ii) use of freshwater for power plant cooling considering once-through, cooling tower or pond technologies; and (iii) availability of precise geographical (latitude-longitude) information. For each power plant, monthly river discharge and water temperature simulations from CWatM-WQ, DynQual and WaterGAP2.2e were extracted from the nearest grid cell (with a maximum of 1 grid cell in each direction) to the power plant location where the

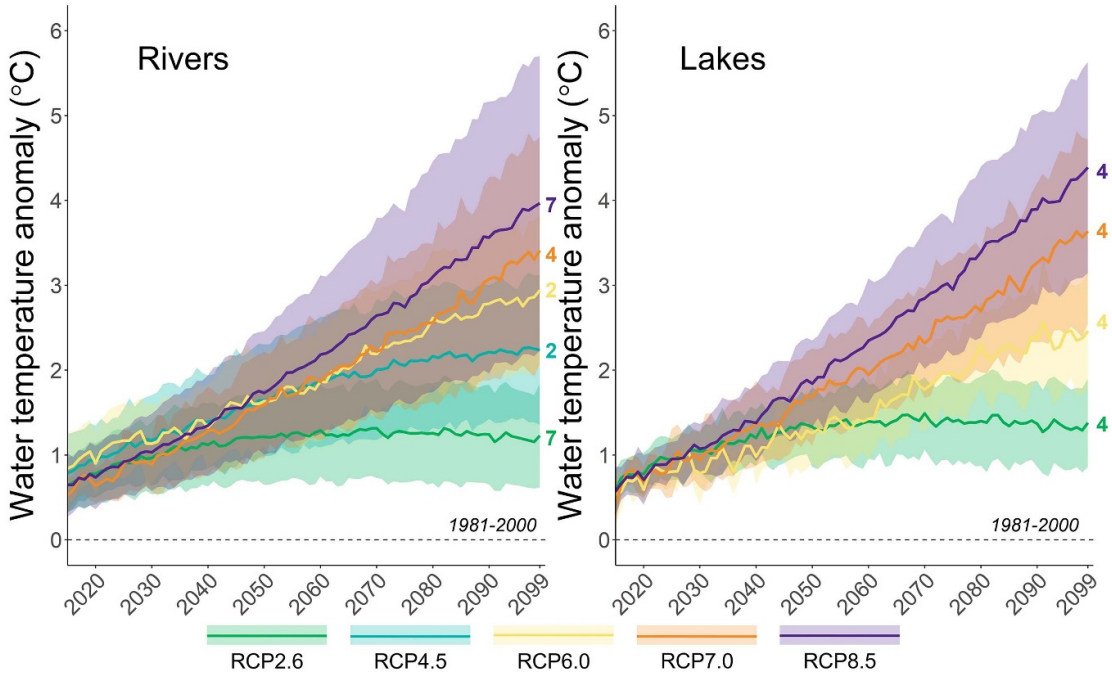

Figure 1. Multi-model ensemble of future global annual surface freshwater temperature anomalies, relative to a historical reference period (1981–2000). Solid lines display the area-weighted arithmetic mean anomaly over all water temperature and global climate models, while shaded areas display the uncertainty as ±1 standard deviation. Coloured numbers display the number of ensemble members per scenario. Ensembles split by ISIMIP round are displayed in supplementary figure S8.

multi-annual monthly average simulated discharge exceeds the average power plant demands. This procedure was necessary to account for spatial mismatches between power plant location and the (assumed) source of cooling water. Where multiple power plants were located in the same grid cell, power plant demands (q) were summed over all power plants prior to calculations of W_{max}.

In total, the installed capacity of all power plants considered is ∼2000 GW, therefore representing around 83% of the global installed capacity of thermoelectric power plants using freshwater (i.e. also including dry and inlet cooling) and roughly 54% of the total installed capacity of all thermoelectric power plants (i.e. also including those cooled by seawater). It should be noted that the location of thermoelectric power plants is not equally distributed across the globe (figure S10), with 96.3% of the installed capacity located in the Northern Hemisphere (table S1).

3. Results

3.1. Multi-model ensembles of future surface water temperature (ISIMIP2b/3b)

Surface freshwater temperatures are projected to rise due to climate change across all water temperature models, GCMs and emission scenarios (figures 1 and 2). Current global average annual water temperatures are already between 0.5 °C–0.8 °C higher than in the reference period (1981–2000). Warming is projected to continue under all future scenarios, largely commensurate with increases in radiative forcing. Relatively small differences between the RCPs are projected up to 2030, with stronger divergence due to climate change under the different scenarios beginning to occur around 2050 and propagating through the second half of the 21st century. The multi-model ensemble for both rivers and lakes shows that, by 2099, global average water temperatures will be approximately +1.3 °C higher than the reference period under RCP2.6, +2.2 °C under RCP4.5, +2.7 °C under RCP6.0, +3.5 °C under RCP7.0 and +4.1 °C under RCP8.5. The spread in water temperature simulations per scenario (figure 1), arising from a combination of different water temperature models and GCMs, is largest under the most extreme climate change scenarios, where models consistently project strong warming but with a large range in water temperature anomalies.

While all models consistently project future increases in surface freshwater temperatures, differences in projections of water temperature anomalies can be substantial (figure 2). The use of climate forcing from different GCMs, even for the same water temperature model, leads to a large range in projected water temperature anomalies. This appears particularly prevalent for both lake (e.g. ALBM, GOTM) and river (e.g. DynQual, WaterGAP3) models forced with CMIP6 (ISIMIP3) climate data, as demonstrated by the spread in min-max water temperature anomalies (figure 2). Anomalies from different water temperature models can

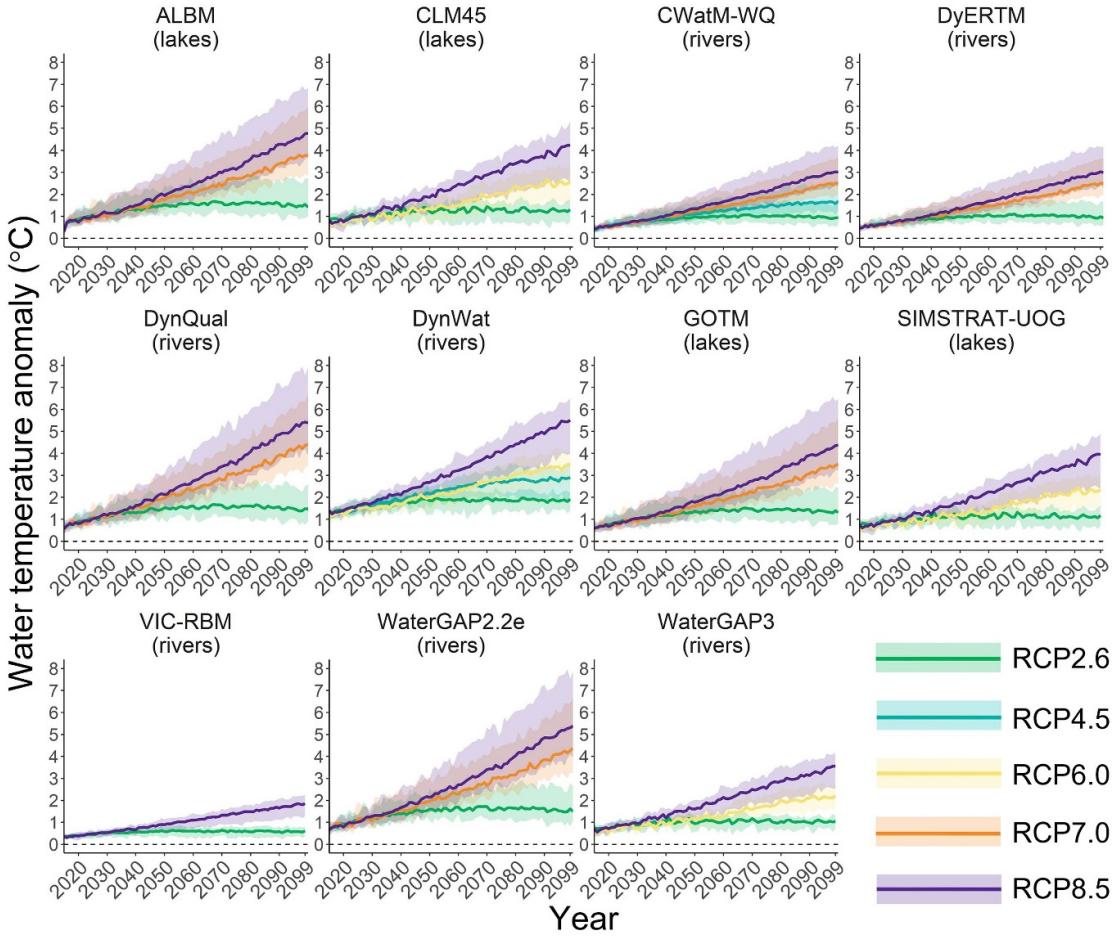

Figure 2. Future global annual surface freshwater temperature anomalies per water temperature model, relative to a historical reference period (1981–2000). Solid lines display the area-weighted arithmetic mean anomaly over all global climate models, while shaded areas display the range over all global climate models as min-max anomalies.

also substantially differ, with (multi-GCM) ensemble averages ranging from around 0.5 °C–1.5 °C for RCP2.6 and 2 °C–5 °C under RCP8.5 by the end of the century.

3.2. Historic river water temperature simulations for 1980–2019 (ISIMIP3a)

Simulated river water temperatures exhibit substantial variation (figures 3 and 4), albeit with a high correlation to the distribution in air temperature (figure S7(a)). However, absolute water temperature simulations can differ substantially between the water temperature models including at global (figure S7(b)) to hemispheric scales (figure 3), and in individual river basins (figure 4).

At the global scale, simulated (area-weighted) river water temperatures display that WaterGAP2.2e is consistently warmest across all parts of the year, with average low temperatures of ∼16 °C in November through February and high temperatures of ∼23 °C in June through August (figure S7(b)). While these patterns are closely replicated by CWatM-WQ and DynQual, both models simulate average global river water temperatures to be substantially (∼3 °C) lower. Containing 68% of the land by area, patterns in the global average river water temperatures are evidently more reflective of conditions in the Northern Hemisphere. Considering the Northern Hemisphere only, monthly patterns simulated by CWatM-WQ, DynQual and WaterGAP2.2e are overall relatively similar (figure 3), albeit DynQual simulates somewhat lower temperatures (∼8 °C) than CWatM-WQ (∼11 °C) and WaterGAP2.2e (∼11 °C) during winter months (December through February) while simulations by WaterGAP2.2e are approximately ∼1 °C higher during the summer months (June through August) than CWatM-WQ and DynQual. Conversely, WaterGAP2.2e consistently simulates higher temperatures (>5 °C) than CWatM-WQ and DynQual in the Southern hemisphere (figure 3).

Patterns in simulated global average water temperatures also vary substantially between individual river basins (figure 4). For example, WaterGAP2.2e consistently simulates substantially higher (∼5 °C) water temperatures than both DynQual and CWatM-WQ in the tropical and sub-tropical areas, including in the Amazon, Niger and Indus rivers. CWatM-WQ, while simulating broadly comparable water temperatures to

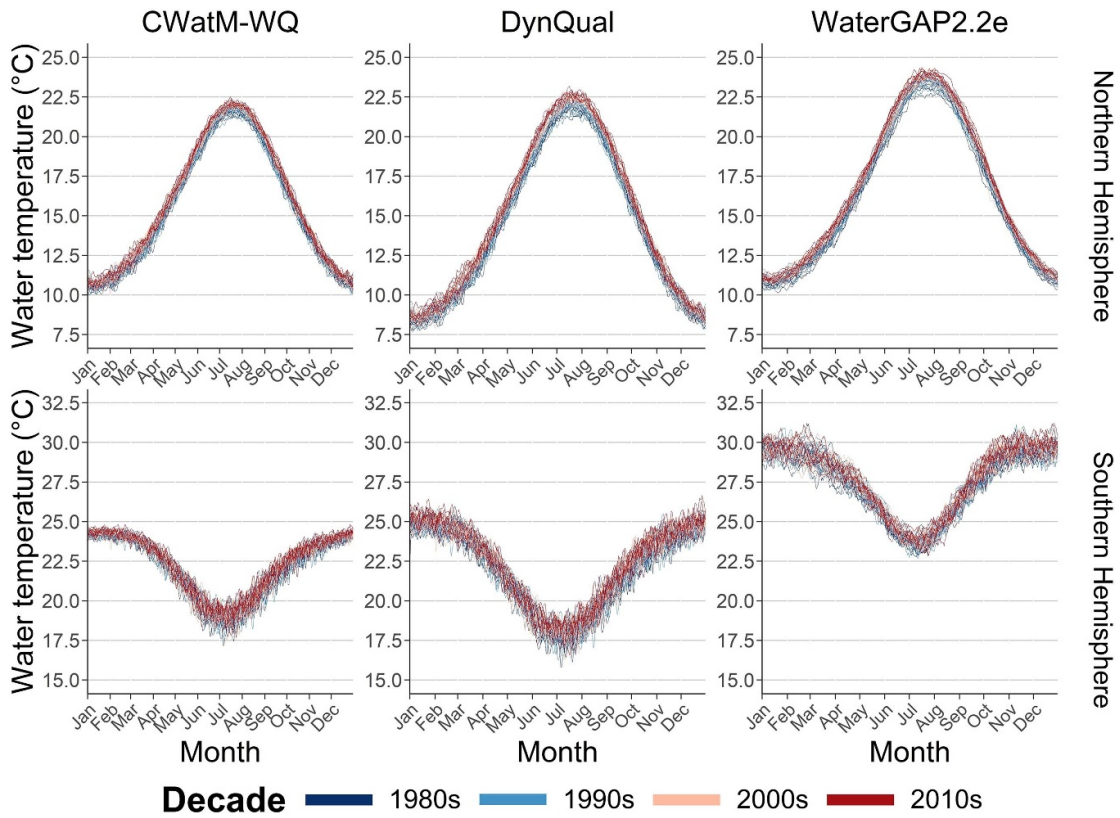

Figure 3. Daily average river water temperatures for the Northern (top) and Southern (bottom) hemispheres; as simulated by CWatM-WQ, DynQual and WaterGAP2.2e for the period 1980–2019. Lines display the daily simulated water temperatures for each year individually, with the line colour indicating the decade.

the other models in the temperate zones (e.g. Loire, Rhine and Danube rivers), simulates slightly lower temperatures than DynQual in the tropical zone but far higher temperatures than both DynQual and WaterGAP2.2e in the northern high-latitudes. These higher water temperatures explain why, despite being largely comparable to DynQual in other world regions, intra-annual variability in the global average water temperature simulated by CWatM-WQ is weaker.

Detailed validation was conducted to further unravel the patterns in river water temperatures amongst the different models (figures S3–S6). For example, the spatial distribution in percentage bias shows that DynQual and WaterGAP2.2e tend to underestimate, and CWatM-WQ overestimate, river water temperatures in high-latitude regions. Outside of the high latitudes, WaterGAP2.2e consistently overestimates water temperature whereas DynQual and CWatM-WQ are more conservative in their simulations—a pattern that is also shown in the global averages (figure S7(a)). Consistent negative biases and KGE values below 0.4 for water temperature simulations in the tropical and sub-tropical zones by CWatM-WQ is reflected back in the river basin temperatures (figure 4), yet is counterbalanced by the overestimates of water temperature at the high latitudes in the global averages (figure 3(a)). Considering the full range of observed versus simulated water temperatures further explains this variability (figure S7). Notably, it can be observed that CWatM-WQ is constrained to simulating water temperatures in the range 3 °C–28 °C (figure S5)—explaining the tendency to overestimate values in high-latitude regions (where observed water temperatures regularly drop below this threshold) and underestimate values in the tropical and sub-tropical regions (where observed water temperatures frequently exceed this water temperature cap). Unlike CWatM-WQ and DynQual, simulations from WaterGAP2.2e can frequently exceed 40 °C which seldom occurs in observational water temperature records.

Despite the models' inherent differences and inter-annual variability, there is high agreement that river water temperatures have already increased with climate change. This is observable in patterns in absolute water temperatures averaged globally (figure S7), per hemisphere (figure 3) and in individual river basins (figure 4), and water temperature anomalies averaged globally (figure 5(a)) and per latitude band (figure 5(b)). Globally averaged anomalies are overall largely consistent, both between the models and throughout the year, with river temperatures on average ∼0.5 °C higher in the 2010s than in the 1980s (figure 5(a)). Of the three models, CWatM-WQ simulates the lowest level of warming with recent climate

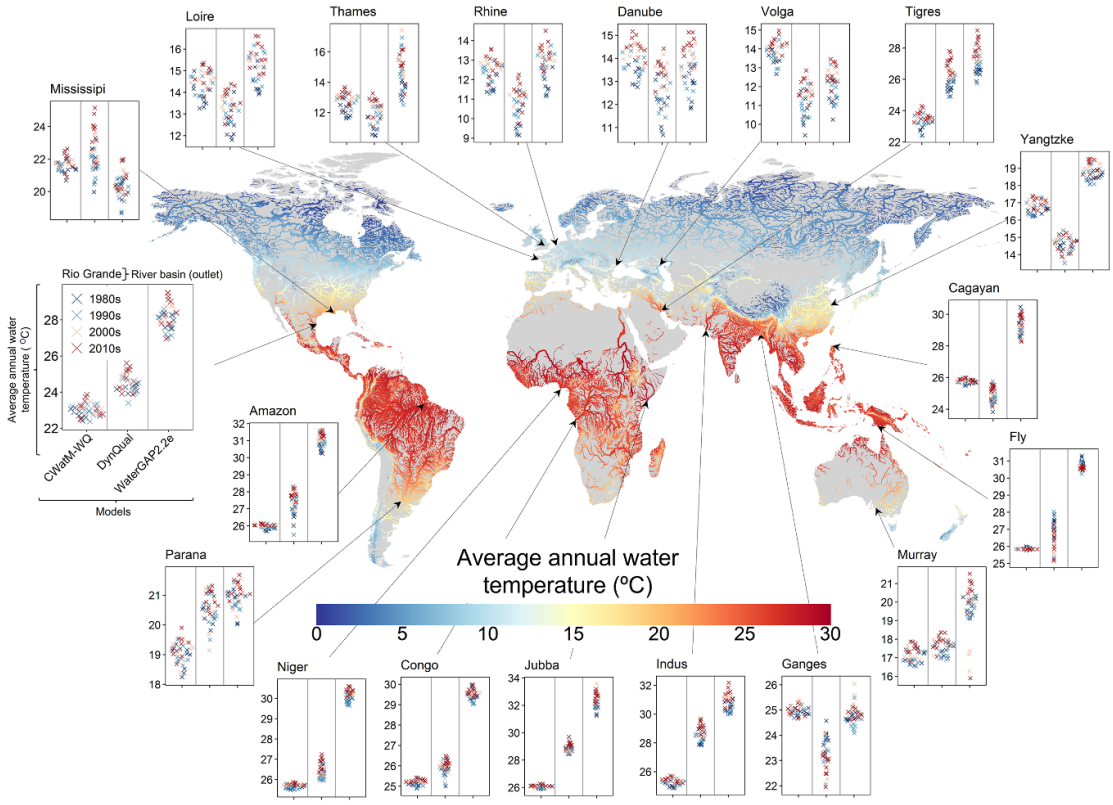

Figure 4. Spatial distribution of annual average water temperatures, based on an ensemble of three river water temperature models (CWatM-WQ, DynQual and WaterGAP2.2e) forced using observed climate data (ISIMIP3a). The map shows the multi-model ensemble average water temperature from 1981–2000 (i.e. the reference period considered in this study), while sinaplots display the average annual water temperature at major river outlets per model between 1980–2019. Each point in the sinaplots represents the average annual water temperature for a given year, while the horizontal spread of points reflects the local density of similar values.

change—particularly in the tropical regions. DynQual and WaterGAP2.2e simulate a similar level of warming due to recent climate change in the tropics, while WaterGAP2.2e consistently simulates water temperature anomalies to be highest in most other world regions (figure 5(b)).

3.3. River water temperature under future climate change (ISIMIP3b)

Consistent with the larger multi-model ensembles (figures 1 and 2), river water temperatures simulated by CWatM-WQ, DynQual and WaterGAP2.2e are projected to substantially increase with future climate change. This is reflected by annual anomalies averaged at the global scale (figure 6(a)), per latitude band (figure 6(b)) and in individual river basins (figure 7), and in monthly anomalies for the Northern and Southern Hemispheres separately (figure 8). The extent of future warming varies strongly across the different scenarios, with the multi-model ensemble projecting average annual global river water temperature to rise by +1 °C, +3.5 °C and +4 °C under SSP1-RCP2.6, SSP3-RCP7.0 and SSP5-RCP8.5, respectively, by the end of the century (figure 6(a)).

DynQual and WaterGAP2.2e exhibit similar warming patterns, both in annual average anomalies averaged globally (figure 6(a)) and per latitude band (figure 6(b)). In the tropics, both models simulated the warming response by 2081–2100 to be around +1 °C, +3.5 °C and +4.5 °C for SSP1-RCP2.6, SSP3-RCP7.0 and SSP5-RCP8.5, respectively. The warming response is somewhat higher under SSP1-RCP2.6, SSP3-RCP7.0 and SSP5-RCP8.5 in the mid-latitudes (+1.5 °C, +4 °C and +5 °C, respectively), yet weaker at the low (+0.5 °C, +2 °C, +2.5 °C, respectively) and high latitudes (+0.8 °C, +2.5 °C, +3 °C, respectively). This is somewhat counterintuitive given that the Arctic is the region with the strongest atmospheric warming, although may be explained by the additional heat input into high latitude rivers and lakes primarily causing melting of ice and snow, whereas in ice-free regions excess energy causes increased warming (Vanderkelen *et al* 2020).

Yet, the uncertainty in the multi-model ensemble is substantial, driven by differences in both the water temperature models and GCMs. For example, while patterns in water temperature simulations from CWatM-WQ are overall consistent with the other models in the mid-latitudes, CWatM-WQ consistently projects warming to occur to a much lesser extent than DynQual or WaterGAP2.2e in the tropical and

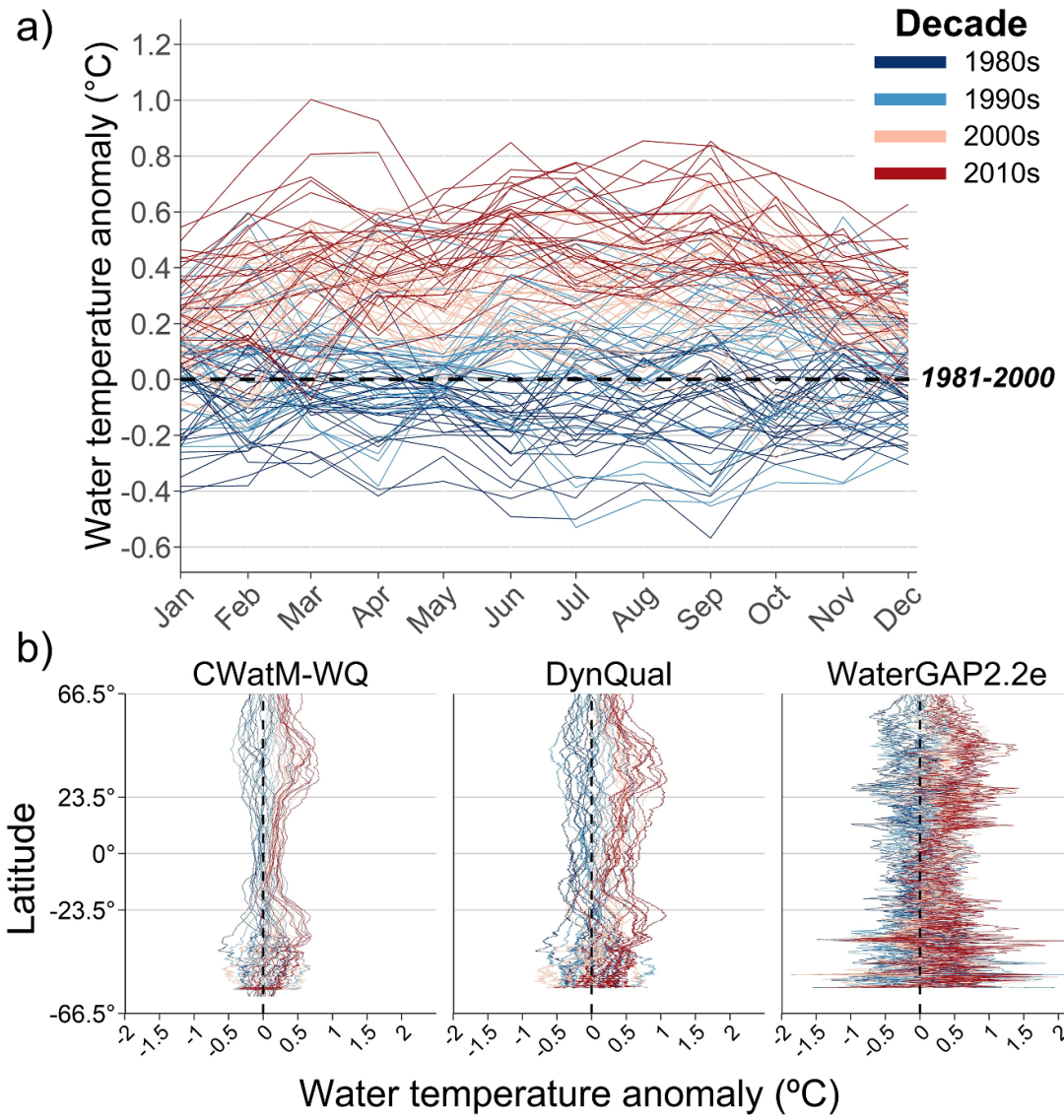

Figure 5. Simulated (a) global (area-weighted) monthly average water temperature anomalies; and (b) annual average water temperature anomalies by latitude; from 1980–2019, with respect to average temperatures over 1981–2000. In all panels, lines display the simulated water temperatures for each year individually, with the line colour indicating the decade.

sub-tropical regions (figure 6(b)). This is driven by the fact that anomalies are dampened for rivers that already approach or exceed the CWatM-WQ's water temperature cap of 28 °C under current climate conditions, as demonstrated in river basins including the Parana, Jubba and Cagayan (figure 7).

Furthermore, even for individual river water temperature models, projected water temperature anomalies can differ substantially due to differences in climate forcing from the GCMs (figures 6(b) and 7). For example, the spread in water temperature anomalies from different GCMs often exceeds the spread from different water temperature models in the mid-latitudes (figure 6(b)), as displayed in the Loire, Parana and Murray rivers (figure 7).

Despite these inherent differences and uncertainties, there is strong agreement that increases in water temperature will occur across all months of the year in both the Northern and Southern Hemispheres with global change (figure 8). Furthermore, all three models suggest that water temperature anomalies will exhibit more pronounced seasonal patterns towards the end-of-the-century—especially under the more pessimistic emissions scenarios (SSP3-RCP7.0 and SSP5-RCP8.5) in the Northern Hemisphere (figure 8). For example, by the end of the century, water temperature anomalies in the Northern Hemisphere are projected to be around +4 °C and +5 °C under SSP3-RCP7.0 and SSP5-RCP8.5 respectively, compared to +1.5 °C under SSP1-RCP2.6. Conversely, monthly patterns appear to remain mostly unchanged in the Southern Hemisphere, with year-round increases of approximately +1 °C, +3 °C and +3.5 °C under SSP1-RCP2.6, SSP3-RCP7.0 and SSP5-RCP8.5, respectively, by the end of the century.

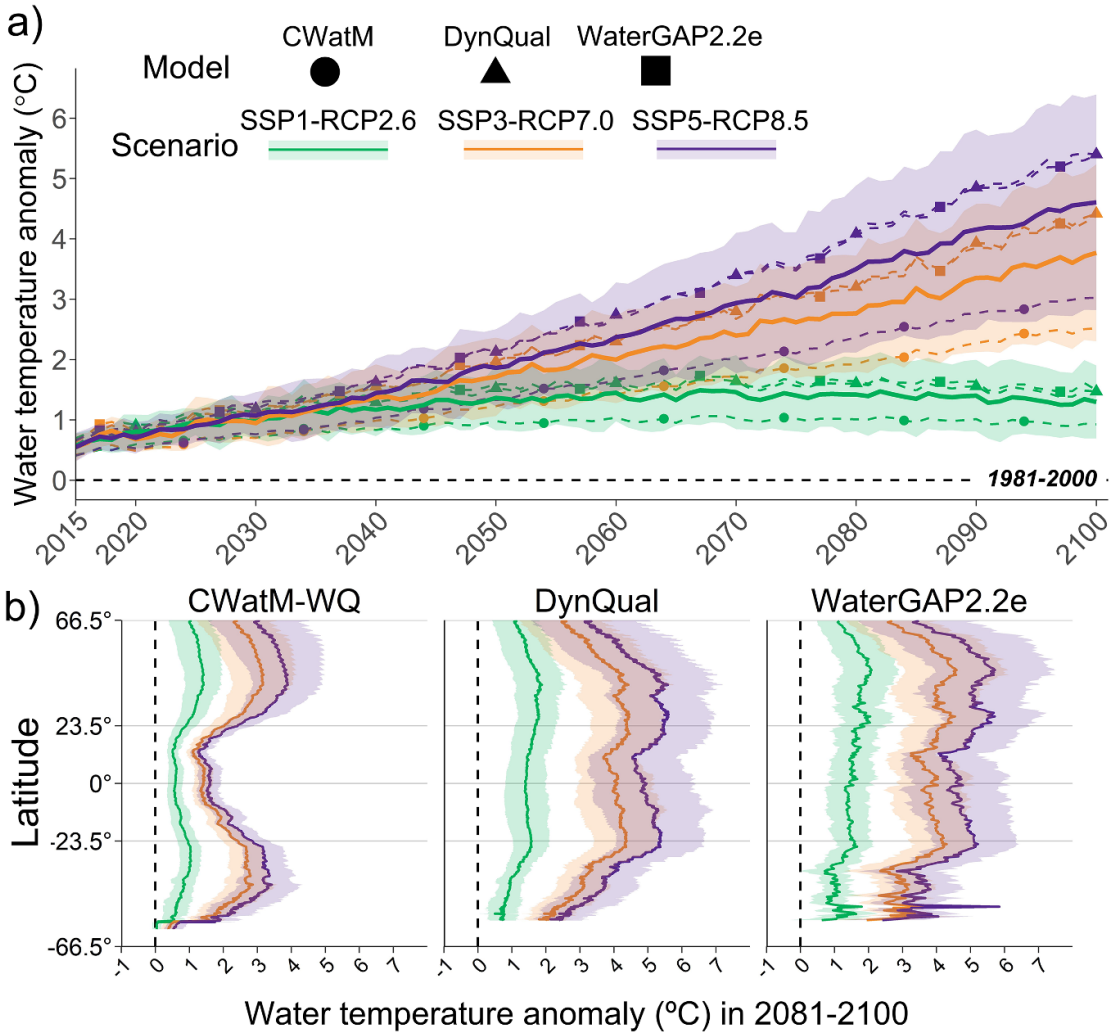

Figure 6. (a) Future global annual surface freshwater temperature anomalies from 2015 to 2100; and (b) water temperature anomalies per latitude at the end of the century (2081–2100). Anomalies are shown under three global change scenarios, relative to the reference period (1981–2000). Solid lines display the area-weighted arithmetic mean anomaly over all water temperature and global climate models, while shaded areas display the uncertainty from a combination of the GCMs and inter-annual variability within the time period as ±1 standard deviation. Dotted lines in panel (a) display the area-weighted arithmetic mean annual anomaly over all global climate models per individual water temperature model. Spatial patterns in absolute average annual water temperatures over 2081–2100 are displayed in supplementary figure S9.

3.4. Power plants feeling the heat?

The annual average usable capacity of existing thermoelectric power plants, which is dependent upon both water availability (i.e. discharge) and water temperature, are estimated at ∼73% (CWatM-WQ); ∼78% (DynQual) and ∼85% (WaterGAP2.2e) of installed capacity over 1980–2019 (figure S11). However, the three models consistently show strong intra-annual variations in usable capacity, which is lowest in summer months in the Northern Hemisphere (May through September) which is where 96.3% of the installed usable capacity is located (table S1, figure S11). While only weak negative trends in annual average usable capacities are observed over 1980–2019 for all models (figure S11(a)), monthly variations over this time period suggest that usable capacities have substantially decreased in the months between May and September in recent decades (e.g. 2010s) compared to the 1980s (figure S11(b)).

Reductions in usable capacity are consistently projected to be substantial under future climate change (figure 9(a)). Compared to 1980–2019, annual average reductions in usable capacity can reach −6% under SSP5-RCP8.5, −4.5% under SSP3-RCP7.0 and −1.5% under SSP1-RCP2.6 by the end of the century (figure 9(a)). Furthermore, there is strong inter-annual variability in reductions across all scenarios, being most acute during the summer months in the Northern Hemisphere. This is particularly significant, as usable capacities are already the lowest in these months in the reference period (figure S11(b)). Additional reductions in thermoelectric usable capacity, primarily driven by increased water temperatures, can therefore lead to a substantial proportion of the installed capacity being unusable. For example, under current conditions for June the multi-model ensemble approximates that 70% of the installed capacity is usable,

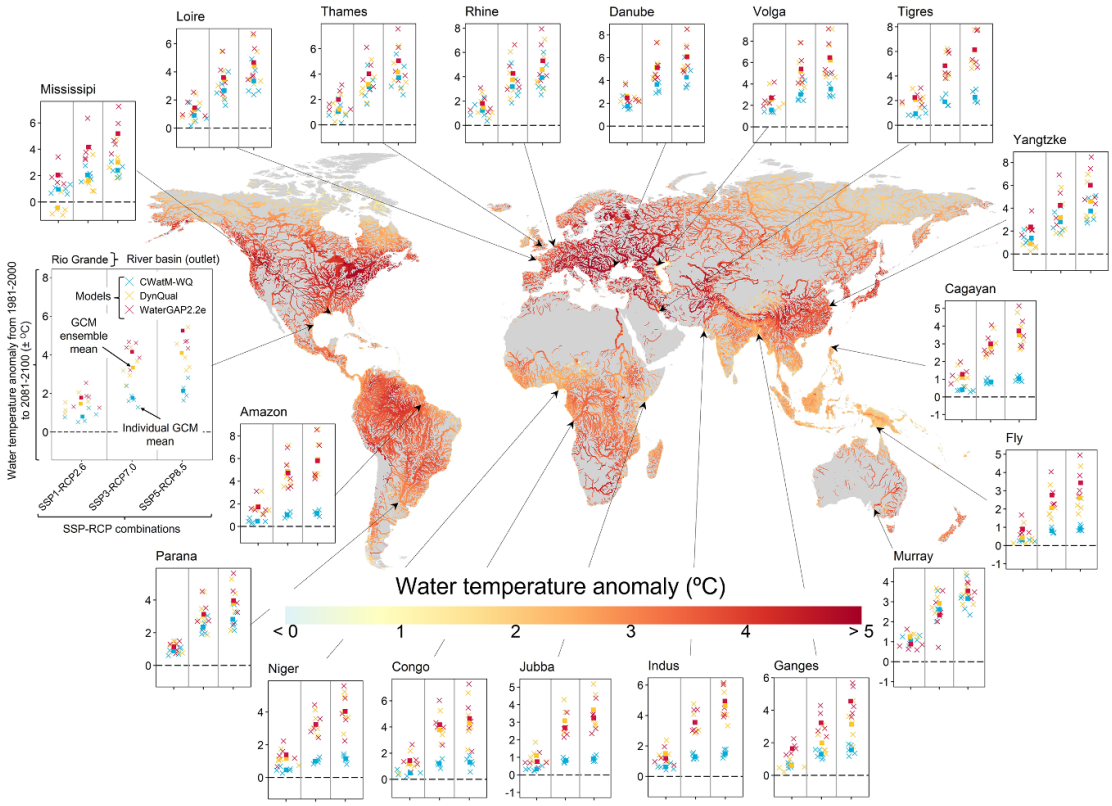

Figure 7. Spatial distribution of annual average water temperature anomalies at the end of the century (2081–2100), relative to a historical reference period (1981–2000), based on an ensemble of three different river water temperature models (CWatM-WQ, DynQual, WaterGAP2.2e) forced using climate data from the five primary global climate models in ISIMIP3b. The map shows the multi-model ensemble average water temperature anomaly under SSP3-RCP7.0, while sinaplots display the average annual water temperature at major river outlets between 2081–2100 per water temperature model and global climate model under three climate change scenarios (SSP1-RCP2.6; SSP3-RCP7.0 and SSP5-RCP8.5).

which is projected to be further reduced by 6% under SSP1-RCP2.6, 11% under SSP3-RCP7.0 and 12.5% under SSP5-RCP8.5 by the end of the century (figure 9(b)). Similar patterns can be observed throughout May to September.

4. Discussion

Global models consistently simulate that surface freshwater temperatures have risen substantially over the last 40 years, with global average annual water temperatures currently 0.5–0.8 °C higher than at the turn of the century (1981–2000). Similarly, warming is consistently projected to continue and intensify under future climatic change—with the multi-model ensemble indicating global annual average water temperature increases of between +1.3–4.1 °C for both rivers and lakes by the end of the century (2081–2100) depending on future scenarios of global change.

Yet, inter-model differences—particularly in absolute water temperature simulations but also in water temperature anomalies—can be substantial. This suggests that a combination of differences in the structure and parameterisation of different water temperature models plays a strong role. For example, most river water temperature models solve the heat advection equation using approaches based on average air temperature as proxies for groundwater heat fluxes, while other models also solve the surface and soil energy balances (e.g. VIC-RBM). Advected heat flux contributions can also differ substantially between models (e.g. inherent differences and inaccuracies in underlying discharge simulations), in addition to differences in how models incorporate hydraulics (e.g. residence times, water velocities). For lake models, differences in the parameterisation of turbulent fluxes, mixing, and ice phenology and configuring the water and sediment columns (e.g. bathymetry and vertical resolution) can contribute significantly to the simulation variability (Golub *et al* 2022). For example, ALBM and CLM45 use the Henderson-Sellers thermal diffusion model for eddy diffusivity parameterisation, whereas GOTM and SIMSTRAT-UOG use the k–ε model. Lastly, water-sediment thermal interactions are included in ALBM and CLM45 but not in GOTM and SIMSTRAT-UOG. While it is beyond the scope of this study to systematically explain the model- and

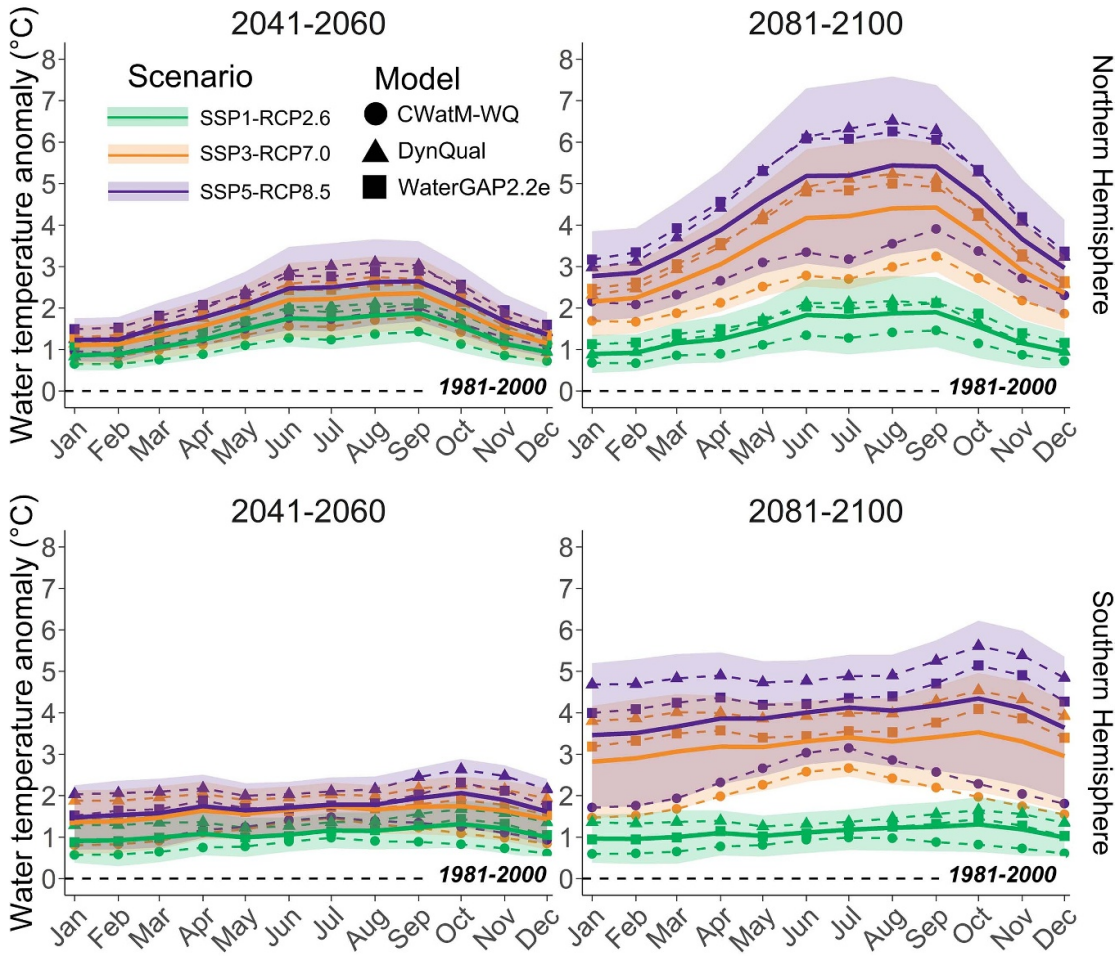

Figure 8. Monthly water temperature anomalies in the Northern (top) and Southern (bottom) hemispheres over 2041–2060 and 2081–2100 under three emissions scenarios, relative to the reference period (1981–2000). Solid lines display the area-weighted arithmetic mean anomaly over all global climate models, while shaded areas display the uncertainty from a combination of the GCMs and inter-annual variability within the time period as ±1 standard deviation.

GCM-specific causes of all these differences, the full range of variability in water temperature simulations can be inferred from figure 2.

Furthermore, water temperature simulations are found to be highly sensitive to the climate forcing from different GCMs. Combining CMIP5 and CMIP6 simulations, which was done for the purpose of generating the largest possible ensemble (figure 1), is also associated with several limitations. For example, CMIP6 models generally exhibit higher climate sensitivity than CMIP5, leading to stronger warming projections for the same radiative forcing (Hausfather *et al* 2022). Additionally, emissions scenarios in CMIP5 and CMIP6, while similar, are not directly interchangeable. Nevertheless, combining CMIP5 and CMIP6 simulations also provides several benefits, such as increasing the number and diversity in climate models included, capturing a wider range of uncertainties in future climate outcomes and allowing for simulations from more impact models to be included.

The differences in model outcomes demonstrate the importance of using an ensemble of water temperature and GCMs to increase the robustness of simulated future changes in water temperature, and to make interpretations less dependent on output from a single model (Trolle *et al* 2014, Golub *et al* 2022). In our analysis, we primarily focus on water temperature anomalies (i.e. differences between future projections and a baseline period). This helps to overcome systematic biases of individual models, for example due to different process representations, which largely cancel out since simulations in both the reference and future periods share a common model structure. When comparing different water temperature models, focusing on anomalies is also advantageous for isolating the signal of climate change from individual model biases, therefore providing more robust assessments of future water temperature changes. Arguably, as ecosystems and infrastructure (e.g. thermoelectric power plants) are typically adapted to the existing water temperature range, the impact of climate-induced water temperature rises are more tied to deviations from current conditions (anomalies).

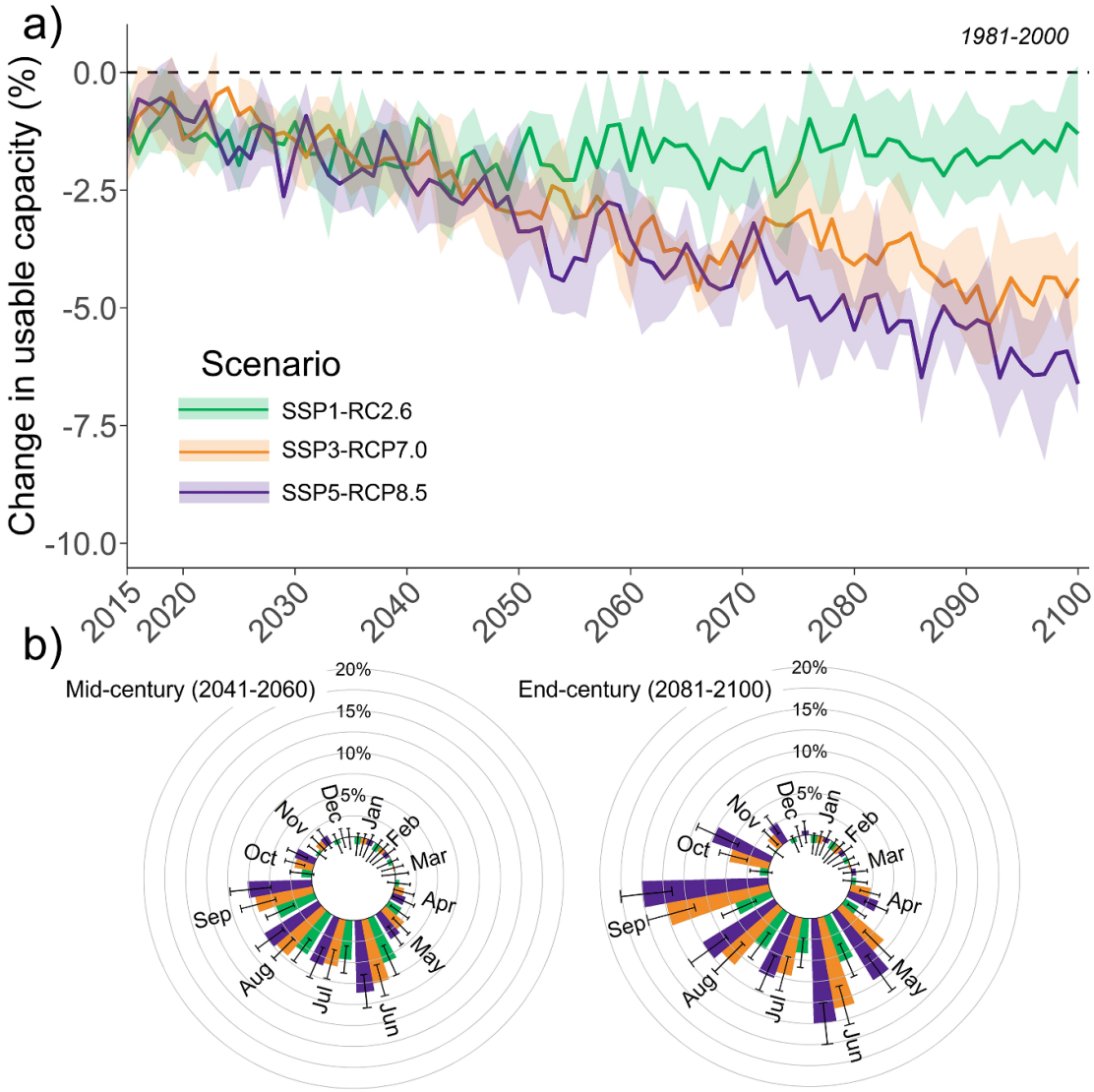

Figure 9. Simulated changes in maximum usable capacity of water-temperature dependent thermoelectric power plants from 2015–2100 from three coupled hydrological and water temperature models, three climate change scenarios and five global climate models. Solid lines in (a) display the multi-model ensemble change in usable capacity based on simulated discharges and river water temperatures. Barplots in (b) display the reduction in monthly maximum usable capacity of power plants for two periods (2041–2060 and 2081–2100) under three climate change scenarios, relative to 1981–2000. Shaded areas in (a) and error bars in (b) display the combined uncertainty resulting from the water temperature model and global climate model as ±1 standard deviation.

Inter-model differences were further explored based on analysis of output from three water temperature models (CWatM-WQ, DynQual and WaterGAP2.2e) which consistently used the same climate forcing for past (ISIMIP3a) and future (ISIMIP3b) conditions. Water temperature models consistently performed best in the temperate zones, as indicated by model performance metrics (figure S3). CWatM-WQ underestimates water temperatures in the tropics and sub-tropics but overestimates values in the high latitude arctic zones due to the model being constrained to only simulate water temperatures between 3 °C and 28 °C. WaterGAP2.2e tends to overestimate water temperatures in most world regions, aside from the high-latitude polar regions which are underestimated. Water temperatures in high-latitude polar regions are also underestimated by DynQual, which is also slightly biased towards lower temperature estimates in the temperate zone.

Water temperature anomalies projected by DynQual and WaterGAP2.2e are largely consistent across all world regions and under the three climate change scenarios, with both models exhibiting strong sensitivity to the climate forcing from different GCMs. Water temperature anomalies projected by CWatM-WQ are comparable to DynQual and WaterGAP2.2e in the temperate zones, but are substantially lower than the

other models in the sub-tropics and tropical zones. This is likely related to the fact that water temperatures in these regions already regularly exceed the 28 °C cap under current climate conditions.

To illustrate a potential impact of projected water temperature rises on society, we estimated the usable capacity of thermoelectric power plants under the three global change scenarios using simulations from CWatM-WQ, DynQual and WaterGAP2.2e. To this end, we only consider the current distribution of thermoelectric power plants that operate with cooling technologies that have a water availability and water temperature dependency. Therefore, the aim of this analysis is not to project usable capacity in the future, but rather to hypothetically explore how our current energy system would fare under future water temperature and discharge regimes (as simulated by multiple coupled hydrological-water temperature models and GCMs).

Direct comparisons with previous studies that have quantified reductions in usable capacity are difficult due to, for example: (i) different spatio-temporal extents and resolutions of analysis; (ii) the use of different climate forcing, scenario assumptions and coupled hydrological-water temperature models; and (iii) definitions of maximum temperature of discharges (Tl_{max}) and the (non)-inclusion of waivers (i.e. regulatory allowances permitting discharges of water at a temperature that exceeds the typical operational limit). Nevertheless, our quantifications of reductions in usable capacity lie within the range of previous assessments, which has been estimated at 2%–12% (USA, by the 2060s) (Liu *et al* 2017), 7.4%–9.5% (Western USA, over 2040–2060) (Bartos and Chester 2015) and 6.7%–19% (Global, in the 2080s) (van Vliet *et al* 2016c).

While our approach for these quantifications is power plant-specific, the global nature of our assessment necessitated broad assumptions and implications. In particular, no global dataset exists for power plant-specific information on the environmental regulations on thermal effluents (Tl_{max}) or compliance contingencies that temporarily relieve power plants from these obligations during extreme conditions. Therefore, and while these factors have a strong impact on quantifications of usable capacity (Liu *et al* 2017), the estimation of some parameters are heavily simplified by quantifying Tl_{max} based on the 95th percentile of water temperature and by allowing power plants to discharge effluent 1 °C warmer than ambient conditions during times of extremely high water temperatures, respectively. Future work to quantify power plant-specific environmental regulations and provisional variances (exemptions) from permit requirements is required to overcome this limitation, facilitating improved estimates of thermoelectric power plant vulnerability to surface water temperature rises under a changing climate. More broadly, future work is required to address the water-energy nexus under global change scenarios more comprehensively—for example, considering various energy transition pathways and their associated water demands and greenhouse gas emissions, demand-side changes and the impact of extreme weather events (e.g. droughts, heatwaves) on the power sector.

5. Conclusion

Both empirical observations and output from water temperature models consistently demonstrate that surface waters globally are already warming. This manifests not only as interruptions at power plants, but for instance also impacts fish species resulting in a shift in the geographical range (Spence and Tingley 2020), altering migration patterns (Otero *et al* 2014) and increasing the likelihood of die-off events (Till *et al* 2019). Models provide a strong basis for understanding global water temperature dynamics and potential impacts under climate change, which is further benefited from using a multi-model ensemble approach. The multi-model ensembles presented in this study strongly indicates that future increases in water temperature are inevitable. While some local adaptation measures exist to control water temperature regimes, such as climate-resilient land-use changes (e.g. restoration of riparian zones) for increasing river shading (Jackson *et al* 2021), cold water releases from existing hydroelectric dams and reservoirs (Olden and Naiman 2010, Null *et al* 2013) or groundwater pumping (Smith and Kurylyk 2024), adaptation options at large scales are limited. Therefore, strong climate change mitigation is crucial for minimising water temperature rises and its associated negative impacts on humankind and ecosystems.

Data availability statement

The data that support the findings of this study are openly available at the following URL/DOI: https://doi.org/10.6084/m9.figshare.28458245.

Acknowledgments

E R J and MTHvV were financially supported by the European Research Council (ERC) under the European Union's Horizon Europe research and innovation program (Grant Agreement 101039426, B-WEX) and the Netherlands Scientific Organisation (NWO) by a VIDI Grant (VI.Vidi.193.019). ERJ acknowledges and thanks the Netherlands Organisation for Scientific Research (NWO) for the Grant that enabled him to use the national supercomputer Snellius (Project: EINF-3999). Z T was supported by the US DOE's Earth System Modelling program through the Energy Exascale Earth System Model (E3SM) project. The Pacific Northwest National Laboratory is operated by Battelle for the U.S. Department of Energy under Contract DE-AC05-76RLO1830. M F acknowledges the project 'Erarbeitung, Testung und pilothafte Anwendung einer integrierten und skalenübergreifenden Analyse- und Bewertungsmethodik der Wasserqualität von Oberflächenund Grundwasser für eine globale, internetbasierte Wasserqualitätsplattform', GlobeWQ (02WGR1 527C), carried out with the support of the Federal Ministry of Education and Research (BMBF) within its research initiative 'Global Resource Water (GRoW)'. A B T has received funding from the European Union's Horizon 2020—Research and Innovation Framework Programme under the H2020 Marie Skłodowska-Curie Actions Grant Agreement No. 956623. W T acknowledges funding from the European Research Council (ERC) under the European Union's Horizon Framework research and innovation programme (Grant Agreement No 101076909; ERC Consolidator Grant 'LACRIMA').

Code and data availability

All code and data required to recreate the findings of this manuscript can be found at: https://figshare.com/s/fac8d92354b33e3653b4 [Note, this is a temporary link—the dataset is currently embargoed and will be made publicly available at 10.6084/m9.figshare.28458245 on acceptance]. All raw water temperature data can be downloaded from the ISIMIP; https://data.isimip.org/.

Conflict of interest

The authors declare no competing interests.

Author contribution

The research was conceptualized by E R J and MTHvV. Water temperature model simulations were provided by Z T (ALBM), W T (CLM45), D F (CWatM-WQ), R K (DyERTM), E R J (DynQual), N W (DynWat), D M B (GOTM), MTHvV (VIC-RBM), H M S (WaterGAP2.2e) and A B T and M F (WaterGAP3). Data processing, analysis, interpretation and write-up was led by E R J. All authors contributed towards and approved the manuscript.

ORCID iDs

Edward R Jones https://orcid.org/0000-0001-5388-7774
Rens van Beek https://orcid.org/0000-0002-4758-108X
Gabriel Cárdenas Belleza https://orcid.org/0000-0002-6003-2288
Peter Burek https://orcid.org/0000-0001-6390-8487
Stephen J Dugdale https://orcid.org/0000-0003-3561-4216
Martina Flörke https://orcid.org/0000-0003-2943-5289
Dor Fridman https://orcid.org/0000-0003-3908-3571
Simon N Gosling https://orcid.org/0000-0001-5973-6862
Rohini Kumar https://orcid.org/0000-0002-4396-2037
Daniel Mercado-Bettin https://orcid.org/0000-0003-4572-3029
Hannes Müller Schmied https://orcid.org/0000-0001-5330-9923
Zeli Tan https://orcid.org/0000-0001-5958-2584
Wim Thiery https://orcid.org/0000-0002-5183-6145
Ammanuel B Tilahun https://orcid.org/0000-0002-2834-5612
Niko Wanders https://orcid.org/0000-0002-7102-5454
Michelle T H van Vliet https://orcid.org/0000-0002-2597-8422

References

Baker E A, Lautz L K, Kelleher C A and Mckenzie J M 2018 The importance of incorporating diurnally fluctuating stream discharge in stream temperature energy balance models *Hydrol. Process.* **32** 2901–14

Barbarossa V, Bosmans J, Wanders N, King H, Bierkens M F P, Huijbregts M A J and Schipper A M 2021 Threats of global warming to the world's freshwater fishes *Nat. Commun.* **12** 1701

Bartos M D and Chester M V 2015 Impacts of climate change on electric power supply in the Western United States *Nat. Clim. Change* **5** 748–52

Büchner S L A 2021 ISIMIP3b bias-adjusted atmospheric climate input data

Delpla I, Jung A-V, Baurès E, Clement M and Thomas O 2009 Impacts of climate change on surface water quality in relation to drinking water production *Environ. Int.* **35** 1225–33

Dugdale S J, Allen Curry R, St-Hilaire A and Andrews S N 2018 Impact of future climate change on water temperature and thermal habitat for keystone fishes in the lower Saint John River, Canada *Water Resour. Manage.* **32** 4853–78

Dugdale S J, Malcolm I A and Hannah D M 2024 Understanding the effects of spatially variable riparian tree planting strategies to target water temperature reductions in rivers *J. Hydrol.* **635** 131163

Eyring V, Bony S, Meehl G A, Senior C A, Stevens B, Stouffer R J and Taylor K E 2016 Overview of the coupled model intercomparison project phase 6 (CMIP6) experimental design and organization *Geosci. Model Dev.* **9** 1937–58

Ficklin D L, Hannah D M, Wanders N, Dugdale S J, England J, Klaus J, Kelleher C, Khamis K and Charlton M B 2023 Rethinking river water temperature in a changing, human-dominated world *Nat. Water* **1** 125–8

Frieler K *et al* 2024 Scenario setup and forcing data for impact model evaluation and impact attribution within the third round of the inter-sectoral impact model intercomparison project (ISIMIP3a) *Geosci. Model Dev.* **17** 1–51

Garner G, Malcolm I A, Sadler J P and Hannah D M 2014 What causes cooling water temperature gradients in a forested stream reach? *Hydrol. Earth Syst. Sci.* **18** 5361–76

Golub M *et al* 2022 A framework for ensemble modelling of climate change impacts on lakes worldwide: the ISIMIP Lake Sector *Geosci. Model Dev.* **15** 4597–623

Goudsmit G-H, Burchard H, Peeters F and Wüest A 2002 Application of k-ϵ turbulence models to enclosed basins: the role of internal seiches *J. Geophys. Res. Oceans* **107** 23-1–13

Grant L *et al* 2021 Attribution of global lake systems change to anthropogenic forcing *Nat. Geosci.* **14** 849–54

Hall A and Selker J S 2021 High-resolution temperature modeling of stream reconstruction alternatives *River Res. Appl.* **37** 931–42

Hannah D M and Garner G 2015 River water temperature in the United Kingdom:Changes over the 20th century and possible changes over the 21st century *Prog. Phys. Geogr.* **39** 68–92

Hausfather Z, Marvel K, Schmidt G A, Nielsen-Gammon J W and Zelinka M 2022 Climate simulations: recognize the 'hot model' problem *Nature* **605** 26–29

Heberling M T, Nietch C T, Thurston H W, Elovitz M, Birkenhauer K H, Panguluri S, Ramakrishnan B, Heiser E and Neyer T 2015 Comparing drinking water treatment costs to source water protection costs using time series analysis *Water Resour. Res.* **51** 8741–56

Isaak D J *et al* 2017 The NorWeST summer stream temperature model and scenarios for the Western U.S.: a crowd-sourced database and new geospatial tools foster a user community and predict broad climate warming of rivers and streams *Water Resour. Res.* **53** 9181–205

Isaak D J, Luce C H, Horan D L, Chandler G L, Wollrab S P and Nagel D E 2018 Global warming of salmon and trout rivers in the Northwestern U.S.: road to Ruin or path through purgatory? *Trans. Am. Fish. Soc.* **147** 566–87

Isaak D J, Young M K, Nagel D E, Horan D L and Groce M C 2015 The cold-water climate shield: delineating refugia for preserving salmonid fishes through the 21st century *Glob. Change Biol.* **21** 2540–53

Jackson F L, Hannah D M, Ouellet V and Malcolm I A 2021 A deterministic river temperature model to prioritize management of riparian woodlands to reduce summer maximum river temperatures *Hydrol. Process.* **35** e14314

Jackson F L, Malcolm I A and Hannah D M 2015 A novel approach for designing large-scale river temperature monitoring networks *Hydrol. Res.* **47** 569–90

Jane S F *et al* 2021 Widespread deoxygenation of temperate lakes *Nature* **594** 66–70

Johnson M F *et al* 2024 Rising water temperature in rivers: ecological impacts and future resilience *WIREs Water* **11** e1724

Jones E R, Bierkens M F P, Wanders N, Sutanudjaja E H, van Beek L P H and van Vliet M T H 2023 DynQual v1.0: a high-resolution global surface water quality model *Geosci. Model Dev.* **16** 4481–500

Jones E R, Graham D J, Van Griensven A, Flörke M and van Vliet M T H 2024 Blind spots in global water quality monitoring *Environ. Res. Lett.* **19** 091001

Kaushal S S, Likens G E, Jaworski N A, Pace M L, Sides A M, Seekell D, Belt K T, Secor D H and Wingate R L 2010 Rising stream and river temperatures in the United States *Front. Ecol. Environ.* **8** 461–6

Koch H and Vögele S 2009 Dynamic modelling of water demand, water availability and adaptation strategies for power plants to global change *Ecol. Econ.* **68** 2031–9

Lee S-Y, Fullerton A H, Sun N and Torgersen C E 2020 Projecting spatiotemporally explicit effects of climate change on stream temperature: a model comparison and implications for coldwater fishes *J. Hydrol.* **588** 125066

Linnerud K, Mideksa T and Eskeland G 2011 The impact of climate change on nuclear power supply *Energy J.* **32** 149–68

Liu L, Hejazi M, Li H, Forman B and Zhang X 2017 Vulnerability of US thermoelectric power generation to climate change when incorporating state-level environmental regulations *Nat. Energy* **2** 17109

Liu Y, Liu J, Ye S, Bureau D P, Liu H, Yin J, Mou Z, Lin H and Hao F 2019 Global metabolic responses of the lenok (Brachymystax lenok) to thermal stress *Comp. Biochem. Physiol. D* **29** 308–19

Lohrmann A, Farfan J, Caldera U, Lohrmann C and Breyer C 2019 Global scenarios for significant water use reduction in thermal power plants based on cooling water demand estimation using satellite imagery *Nat. Energy* **4** 1040–8

Loinaz M C, Davidsen H K, Butts M and Bauer-Gottwein P 2013 Integrated flow and temperature modeling at the catchment scale *J. Hydrol.* **495** 238–51

Martí-Cardona B, Prats J and Niclòs R 2019 Enhancing the retrieval of stream surface temperature from Landsat data *Remote Sens. Environ.* **224** 182–91

Mcdermott G R and Nilsen Ø A 2014 Electricity prices, river temperatures, and cooling water scarcity *Land Econ.* **90** 131–48

Michel A, Schaefli B, Wever N, Zekollari H, Lehning M and Huwald H 2022 Future water temperature of rivers in Switzerland under climate change investigated with physics-based models *Hydrol. Earth Syst. Sci.* **26** 1063–87

Mohseni O and Stefan H G 1999 Stream temperature/air temperature relationship: a physical interpretation *J. Hydrol.* **218** 128–41

Morrill J C, Bales R C and Conklin M H 2005 Estimating stream temperature from air temperature: implications for future water quality *J. Environ. Eng.* **131** 139–46
Müller Schmied H *et al* 2024 The global water resources and use model WaterGAP v2.2e: description and evaluation of modifications and new features *Geosci. Model Dev.* **17** 8817–52
Nicola G G, Elvira B, Jonsson B, Ayllón D and Almodóvar A 2018 Local and global climatic drivers of Atlantic salmon decline in southern Europe *Fish. Res.* **198** 78–85
Null S E, Ligare S T and Viers J H 2013 A method to consider whether dams mitigate climate change effects on stream temperatures *JAWRA J. Am. Water Resour. Assoc.* **49** 1456–72
O'Reilly C M *et al* 2015 Rapid and highly variable warming of lake surface waters around the globe *Geophys. Res. Lett.* **42** 10,773–81
Olden J D and Naiman R J 2010 Incorporating thermal regimes into environmental flows assessments: modifying dam operations to restore freshwater ecosystem integrity *Freshw. Biol.* **55** 86–107
Oleson K W, Lawrence D M, Bonan G B, Drewniak B, Huang M, Koven C D, Levis S, Li F, Riley W J and Subin Z M 2013 Technical description of version 4.0 of the community land model (CLM) *NCAR Tech. Note NCAR/TN-478+ STR* vol 257 pp 1–257
Otero J *et al* 2014 Basin-scale phenology and effects of climate variability on global timing of initial seaward migration of Atlantic salmon (Salmo salar) *Glob. Change Biol.* **20** 61–75
Petrakopoulou F, Robinson A and Olmeda-Delgado M 2020 Impact of climate change on fossil fuel power-plant efficiency and water use *J. Clean. Prod.* **273** 122816
Platts U 2012 UDI world electric power plants data base March 2012
Pohle I, Helliwell R, Aube C, Gibbs S, Spencer M and Spezia L 2019 Citizen science evidence from the past century shows that Scottish rivers are warming *Sci. Total Environ.* **659** 53–65
Ptak M, Sojka M, Kałuża T, Choiński A and Nowak B 2019 Long-term water temperature trends of the Warta River in the years 1960–2009 *Ecohydrol. Hydrobiol.* **19** 441–51
Punzet M, Voß F, Voß A, Kynast E and Bärlund I 2012 A global approach to assess the potential impact of climate change on stream water temperatures and related in-stream first-order decay rates *J. Hydrometeorol.* **13** 1052–65
Raptis C E and Pfister S 2016 Global freshwater thermal emissions from steam-electric power plants with once-through cooling systems *Energy* **97** 46–57
Rincón E, St-Hilaire A, Bergeron N E and Dugdale S J 2023 Combining Landsat TIR-imagery data and ERA5 reanalysis information with different calibration strategies to improve simulations of streamflow and river temperature in the Canadian Subarctic *Hydrol. Process.* **37** e15008
Smith K A and Kurylyk B L 2024 Pumping groundwater to create cold-water thermal refuges in warming rivers *Ecohydrology* **18** e2739
Spence A R and Tingley M W 2020 The challenge of novel abiotic conditions for species undergoing climate-induced range shifts *Ecography* **43** 1571–90
Tan Z, Yao H, Melack J, Grossart H-P, Jansen J, Balathandayuthabani S, Sargsyan K and Leung L R 2024 A lake biogeochemistry model for global methane emissions: model development, site-level validation, and global applicability *J. Adv. Model. Earth Syst.* **16** e2024MS004275
Tavares M H, Cunha A H F, Motta-Marques D, Ruhoff A L, Fragoso C R, Munar A M and Bonnet M-P 2020 Derivation of consistent, continuous daily river temperature data series by combining remote sensing and water temperature models *Remote Sens. Environ.* **241** 111721
Taylor K E, Stouffer R J and Meehl G A 2012 An overview of CMIP5 and the experiment design *Bull. Am. Meteorol. Soc.* **93** 485–98
Till A, Rypel A L, Bray A and Fey S B 2019 Fish die-offs are concurrent with thermal extremes in north temperate lakes *Nat. Clim. Change* **9** 637–41
Trolle D, Elliott J A, Mooij W M, Janse J H, Bolding K, Hamilton D P and Jeppesen E 2014 Advancing projections of phytoplankton responses to climate change through ensemble modelling *Environ. Modelling Softw.* **61** 371–9
Umlauf L and Burchard H 2005 Second-order turbulence closure models for geophysical boundary layers. A review of recent work *Cont. Shelf Res.* **25** 795–827
van Vliet M T H, van Beek L P H, Eisner S, Flörke M, Wada Y and Bierkens M F P 2016a Multi-model assessment of global hydropower and cooling water discharge potential under climate change *Glob. Environ. Change* **40** 156–70
van Vliet M T H, Sheffield J, Wiberg D and Wood E 2016b Impacts of recent drought and warm years on water resources and electricity supply worldwide *Environ. Res. Lett.* **11** 124021
van Vliet M T H, Wiberg D, Leduc S and Riahi K 2016c Power-generation system vulnerability and adaptation to changes in climate and water resources *Nat. Clim. Change* **6** 375–80
van Vliet M T H, Yearsley J R, Franssen W H P, Ludwig F, Haddeland I, Lettenmaier D P and Kabat P 2012b Coupled daily streamflow and water temperature modelling in large river basins *Hydrol. Earth Syst. Sci.* **16** 4303–21
van Vliet M T H, Yearsley J, Ludwig F, Vögele S, Lettenmaier D and Kabat P 2012a Vulnerability of US and European electricity supply to climate change *Nat. Clim. Change* **2** 676–81
Vanderkelen I *et al* 2020 Global Heat Uptake by Inland waters *Geophys. Res. Lett.* **47** e2020GL087867
Wanders N, van Vliet M T H, Wada Y, Bierkens M F P and Van Beek L P H 2019 High-resolution global water temperature modeling *Water Resour. Res.* **55** 2760–78
Wehrly K E, Wang L and Mitro M 2007 Field-based estimates of thermal tolerance limits for trout: incorporating exposure time and temperature fluctuation *Trans. Am. Fish. Soc.* **136** 365–74
Wolf D, Georgic W and Klaiber H A 2017 Reeling in the damages: harmful algal blooms' impact on Lake Erie's recreational fishing industry *J. Environ. Manage.* **199** 148–57
Woolway R I *et al* 2021 Phenological shifts in lake stratification under climate change *Nat. Commun.* **12** 2318
Woolway R I, Weyhenmeyer G A, Schmid M, Dokulil M T, De Eyto E, Maberly S C, May L and Merchant C J 2019 Substantial increase in minimum lake surface temperatures under climate change *Clim. Change* **155** 81–94
Worrall F, Howden N J K, Burt T P and Hannah D M 2022 River water temperature demonstrates resistance to long-term air temperature change *Hydrol. Process.* **36** e14732
Zhu S, Luo Y, Graf R, Wrzesiński D, Sojka M, Sun B, Kong L, Ji Q and Luo W 2022 Reconstruction of long-term water temperature indicates significant warming in Polish rivers during 1966–2020 *J. Hydrol.* **44** 101281